JOURNAL OF BACTERIOLOGY, May 1978, p. 423-433
0021-9193/78/0134-0423$02.00/0

Vol. 134, No. 2
Printed in U.S.A.

Size Variations and Correlation of Different Cell Cycle Events in Slow-Growing *Escherichia coli*

LUUD J. H. KOPPES, CONRAD L. WOLDRINGH,* AND NANNE NANNINGA

Department of Electron Microscopy and Molecular Cytology, University of Amsterdam, Amsterdam, The Netherlands

Received for publication 10 November 1977

Cell lengths have been determined at which cell cycle events occur in the slow-growing *Escherichia coli* B/r substrains A, K, and F26. The radioautographic and electron microscope analyses allowed determination of the variation in length at birth, initiation and termination of DNA replication, and initiation of the constriction process and of cell separation. In all three substrains the standard deviation increased between cell birth and initiation of DNA replication. From there on, the standard deviation remained relatively constant until cell separation. These observations are consistent with the presence of a deterministic phase during the cell cycle in which the cell sizes at initiation of DNA replication and at cell division are correlated.

In a bacterial population growing under steady-state conditions, cells divide in such a way that the variation of cell sizes at division remains relatively small and constant in time (14). In addition, every newborn cell receives one of the two replicated daughter chromosomes. Because of this apparent precision, the coordination of DNA replication with respect to cell elongation and cell division has obtained special attention in studies on the bacterial cycle (3, 6). For instance, models have been presented in which it is assumed that a rod-shaped bacterium like *Escherichia coli* elongates at a constant rate proportional to a fixed number of envelope growth zones, which double at a particular time in the cell cycle (4, 29). The time of doubling in rate of elongation was supposed to coincide with initiation (4, 26) or termination (8, 23, 28) of DNA replication. Such a doubling in the rate of envelope synthesis could induce cell division a definite time later, for instance, when the suitable surface-to-volume ratio has been reached (21, 22). So far, however, experiments in which volume increase or elongation was monitored after inhibition of DNA synthesis (5, 26) or after alteration of the replication rate (A. Zaritsky and C. L. Woldringh, manuscript in preparation) have failed to reveal a correlation between cell growth and DNA replication.

A different approach to gain insight into the possible correlation between a particular event of the cell cycle and cell division has been presented by Koch (13). He observed (14) and emphasized (13) that cell size at division is regulated in a relatively precise way, the coefficient of variation in cell size at division being about half the coefficient of variation in cell age. This requires, according to Koch (13), that the point of control in the cell cycle which determines cell division must occur with at least the same coefficient of variation with respect to cell size.

We have determined in *E. coli* the variations in size of cells engaged in initiation and termination of DNA replication as well as in initiation of the cell constriction process. The radioautographic and electron microscope analyses were performed on three different substrains of *E. coli* B/r in which the above events have been shown to occur at different times during the cycle under conditions of slow growth (12, 27). The results suggest the occurrence of a deterministic phase in the cell cycle in which, after initiation of chromosome replication, the cells proceed in an orderly sequence towards division.

MATERIALS AND METHODS

Bacterial strains and growth conditions. The organisms used were *E. coli* B/r A (ATCC 12407), *E. coli* B/r F26 *thy his*, obtained from C. E. Helmstetter, and *E. coli* B/r K, obtained from H. Kubitschek. They were grown in the minimal medium used by Helmstetter and Cooper (11) with 0.08% L-alanine or with a mixture of 0.04% L-alanine and 0.04% L-proline as the carbon source. When grown in the same medium, the doubling time (τ) of *E. coli* B/r A was about two-thirds that of *E. coli* B/r K (see Table 1 in ref. 27). In experiments with *E. coli* B/r F26 *thy his*, 10 μg of thymine and 50 μg of L-histidine were added per ml. For each experiment, 100 ml of minimal medium was inoculated with bacteria and incubated under aeration by shaking in a water bath at 37°C. After 16 to 20 h of incubation, i.e., after about the tenth generation, growth was monitored by measuring with a Gilford spectrophotometer the absorbance at 450 nm

in samples fixed with 0.3% formaldehyde. In some experiments, the cell concentration was measured in a model Z_B Coulter Counter equipped with a 30-μm aperture.

Pulse-labeling with [^{3}H]thymidine. When the absorbance had reached a value of 0.3 to 0.4, 40 ml of culture was rapidly filtered (Millipore Corp., Bedford, Mass.; filter diameter, 47 mm; pore size, 0.45 μm), washed with 100 ml of fresh, prewarmed growth medium, and resuspended in 4 ml of the same medium. Samples of 0.5 ml of this suspension were added to [^{3}H]thymidine (obtained from the Radiochemical Centre, Amersham, England; final concentration, 50 μCi/ml, i.e., 0.24 μg/ml) and adenosine (250 μg/ml; ref. 18) and incubated at 37°C for 5% of the doubling time. The incorporation was stopped by adding 10 volumes of ice-cold minimal salts medium supplemented with 0.5 mg of thymidine per ml and, subsequently, 1 volume of ice-cold OsO_4 (0.1% final concentration). Samples in which the incorporation was stopped immediately after adding them to the [^{3}H]thymidine served as controls for aspecific grains in the radioautograms (less than 0.2 grain per cell). Finally, the cells were sedimented by centrifugation at 6,000 × *g* for 15 min at 4°C, washed with minimal salts medium supplemented with 0.5 mg of thymidine per ml, and resuspended in minimal salts medium with 0.1% OsO_4.

Agar filtration and radioautography. Agar filtration was carried out as previously described (27). For radioautography, the plastic film with adhering bacteria was floated off on distilled water. It was picked up from below with a glass slide previously covered with a collodion membrane. The slides were dipped with a semiautomatic apparatus in Ilford L4 emulsion, diluted with 2 volumes of distilled water, at 32°C (16). Checks were made in the electron microscope to establish the homogeneous distribution of silver bromide crystals. After an exposure for 2 weeks, the slides were developed for 7 min in Agfa-Gevaert developer preceded by 1 min of gold latensification (17). The radioautograms were transferred to electron microscope grids, and areas were photographed at random with a Philips EM 300 electron microscope.

Analysis of radioautograms. The length of cells was measured, and the overlying grains were counted from projections of the negatives on a transparent screen at a final magnification of ×12,000. The number of radioactive cells in each length class was calculated by a computer (model HP g825) according to the procedure suggested by Koch (13), which involves a Poisson analysis of the distribution of grain counts per cell. In the total population, a subpopulation with a low average number of grains characteristic of cells not synthesizing DNA and a subpopulation with a higher average number of grains characteristic of cells synthesizing DNA could be distinguished. From these two averages and the observed distribution of grain counts in each length class, the fraction of cells engaged in DNA synthesis was calculated. Details of the computer program have been published elsewhere (15).

Symbols. Symbols used for the different parameters of the cell cycle are listed in Table 1.

RESULTS

Comparison of length distributions of control cells and cells treated for radioautography. Most of the length distributions obtained from untreated control cells (Fig. 1, continuous line) were found to differ significantly from those of the radioautograms, as indicated by the Kolmogorov-Smirnov test (24) applied at a level of significance of $\alpha = 0.10$. Application and development of the emulsion can be assumed to cause aspecific shrinkage or expansion of the cells in radioautograms, resulting in deviations with respect to average cell length from the control population. Therefore, the lengths of cells from radioautograms were corrected by multiplication with the ratio between the average lengths of the two populations (correction factor *f*, in Table 2). After this correction, the cumulative distributions of radioautographed cells coincided with those of control cells (Fig. 2A and B). Furthermore, a decrease in the percentage of constricted cells was observed when they had been covered with emulsion for radioautography. This decrease may be ascribed to a masking effect by the emulsion, especially in newly initiated constrictions. This interpretation is supported by the absence of short constricted cells in radioautograms (data not shown). Because of these possible artifacts, all subsequent data on cells showing constriction have been taken from control populations (solid lines and speckled areas in Fig. 1A and B).

TABLE 1. *Symbols used for different parameters of the cell cycle*

Event	Symbols for (at event): Avg length	Frequency distribution of length	Cumulative frequency distribution of length	Relative age	Period between	
Birth	L_o	ψ	Ψ	a_o		
Initiation of DNA replication	L_i	ω	Ω	a_i	B	
Termination of DNA replication	L_t	θ	Θ	a_t	C	τ
Initiation of cell constriction	L_{ci}[a]	γ	Γ	a_{ci}	T	D
Separation of daughters	L_s	ϕ	Φ	a_s		

[a] Not to be confused with the average length of constricted cells ($\bar{L}_c$ in Table 2).

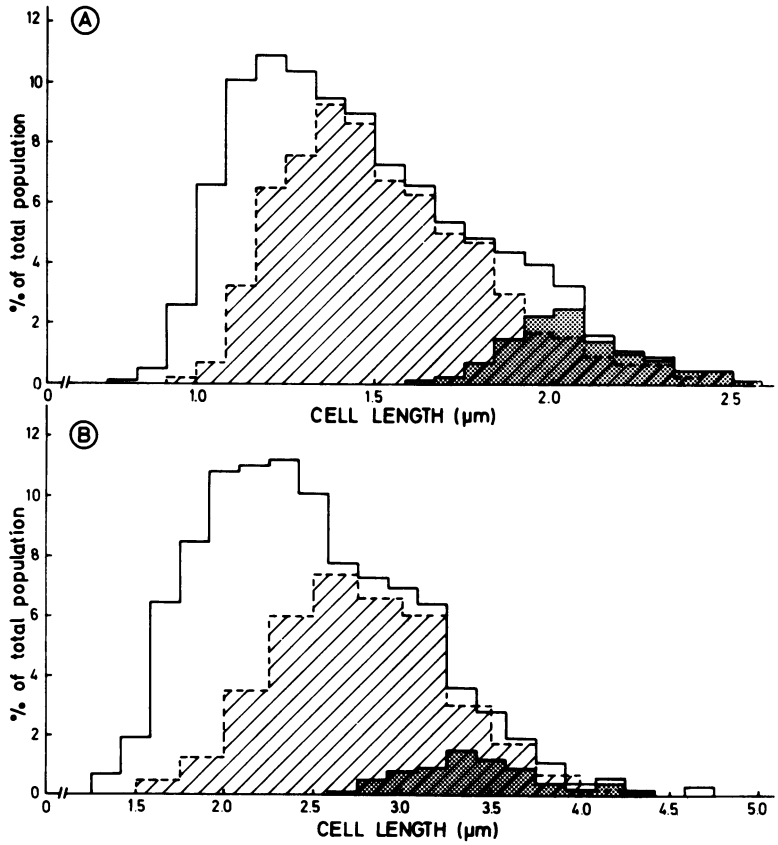

FIG. 1. *Length distributions of E. coli B/r A and K prepared by agar filtration. (A) E. coli B/r A; τ = 109 min. (B) E. coli B/r K; τ = 100 min. Note the use of different length scales. Speckled area: distribution of constricted cells in the total population of the control (continuous line; treatment A in Table 2). Hatched area: distribution of radioactive cells in the population pulse-labeled with [^{3}H]thymidine and subjected to radioautography (treatment B in Table 2).*

For the combined populations, the average length of separating cells (vertical lines L_s in Fig. 2) has been calculated from the average length of the control population and from its coefficient of variation (see Table 2) by comparison with the parameters for theoretical distributions given by Koch (Table 4 in ref. 13). Almost identical L_s values were obtained when applying the formula of Harvey et al. (10): $L_s = L_{min} + 1/2\ L_{max}$, where L_{min} and L_{max} are, respectively, the minimal and maximal cell lengths observed in the distribution.

Cumulative distributions of cells which initiate or terminate DNA replication. The length distributions of radioactive cells observed in radioautograms of *E. coli* B/r A and K are indicated by the hatched areas in Fig. 1A and B. It is evident that B/r K cells become radioactive at a relatively larger length in the cell cycle than B/r A cells. In Fig. 2A and B, DNA replicating cells found in the radioautograms have been plotted as the percentage of radioactive cells per length class. It can be seen that these percentages increase as a function of cell length from about 15 to 97% in *E. coli* B/r A, and from 0 to 95% in strain B/r K. This increase can be considered to represent the cumulative length distribution of the population of cells that initiate DNA replication, whereas the subsequent decrease in the percentage of radioactive cells per length class can be considered to result from completion of DNA replication. In contrast to B/r K cells, a second increase was found in B/r A cells at the end of the cycle (Fig. 2A). We interpret the radioactivity in these cells as resulting from reinitiation of DNA replication within the same cycle. These particular cells can be distinguished in the radioautograms as constricted cells with about twice the number of grains found for the average radioactive cell. Therefore, these cells were scored as unlabeled when estimating the percentage of cells per

TABLE 2. *Parameters of length distributions obtained from control and radioautographed cells*

Strain	τ[a] (min)	Treatment	No. of cells measured	$\bar{L}$ (μm)	CV[b] (%)	f[c]	Constricted cells (%)	L_s[d] (μm)	$\bar{L}_c$[e] (μm)	CV (%)
B/r A	109	A[f]	1,549	1.47	22.6	1.00	10.5	2.1	2.0	8.4
		B[g]	3,163	1.53	23.4	0.96	6.9		2.2	8.4
B/r A	135	A	956	1.43	22.3	1.00	8.1	2.1	2.1	8.2
		B	1,879	1.47	21.9	0.97	7.7		2.1	8.0
B/r K	100	A	1,396	2.49	24.0	1.00	7.1	3.6	3.4	11.0
		B	3,155	2.40	26.4	1.04	5.1		3.5	11.9
B/r K	210	A	970	2.00	24.0	1.00	5.7	3.0	3.0	10.1
		B	940	2.09	22.3	0.96	3.6		2.9	9.9
B/r F26	240	B	2,545	1.49	23.7	1.00	8.1	2.2	2.1	11.1

[a] The different doubling times were obtained by the use of alanine plus proline (τ = 100) or alanine (τ = 109, 135, 210, and 240) as carbon source.
[b] CV, Coefficient of variation.
[c] f, Correction factor. $f = \bar{L}$ of the control cells/$\bar{L}$ of the radioautographed cells.
[d] L_s, Average length of separating cells.
[e] $\bar{L}_c$, Average length of cells showing constriction.
[f] A, Untreated control cells.
[g] B, Cells pulse-labeled with [^{3}H]thymidine and covered with emulsion for radioautography.

length class that are radioactive as a result of the first round of DNA replication. The cumulative length distribution of cells which terminate DNA replication can now be calculated for both strains after taking into consideration (i) the small percentage of cells per length class that have not yet initiated DNA replication (see Appendix, part i), and (ii) the percentage of cells that disappeared from every length class because they had already proceeded through cell separation (see Appendix, part ii). In Fig. 2C and D, the cumulative length distributions of cells that initiate or terminate chromosome replication have been plotted on probability paper. Assuming that cell length at initiation or termination is normally distributed, the average lengths at initiation (L_i) or termination (L_t) and their standard deviations (SD) can be derived from the calculated regression lines.

Cumulative distributions of separating and newborn cells and of cells which initiate cell constriction. To perform the correction for depletion of length classes as a result of cell separation (Appendix, part ii), the length distribution of separating cells has to be known. The only experimental observation that refers to this distribution is the one of constricted cells in the control population ($\bar{L}_c$ in Table 2). This distribution represents both the process of cell separation and that of cell constriction. It will therefore be more dispersed than the distribution of separating cells alone, because cells continue to elongate during constriction (see below). The distribution of separating cells has been assumed to be Gaussian with an average at L_s and a coefficient of variation equal to that of the distribution of constricted cells. It is represented in cumulative form by the dashed lines in Fig. 2C and D.

Cumulative distributions of newborn cells have been drawn in Fig. 2C and D assuming that the average length (L_o) is equal to 1/2 L_s and that the coefficient of variation is equal to that of the distribution of the daughters of the constricted cells. A similar cumulative distribution of newborn cells (crosses in Fig. 2C and D) is obtained when making use of the distribution of the ratio between lengths of daughter and mother cells (10, 20), as shown in Fig. 3. From this figure it can be noted that the longer and thinner B/r K cells divide less precisely (coefficient of variation, 9%) than the shorter and thicker B/r A cells (coefficient of variation, 5%).

By calculating the percentage of constricted cells per length class (Fig. 2A and B), the cumulative distribution of cells at the start of the constriction process can be obtained after correction for depletion of length classes as a result of cell separation. The average of this distribution gives the length, L_{ci}, at which cell constriction is initiated (Fig. 2C and D).

Average lengths and SD of different parameters in the cell cycle. In Table 3 the relative average lengths and SD, derived as described in Fig. 1 and 2, have been summarized

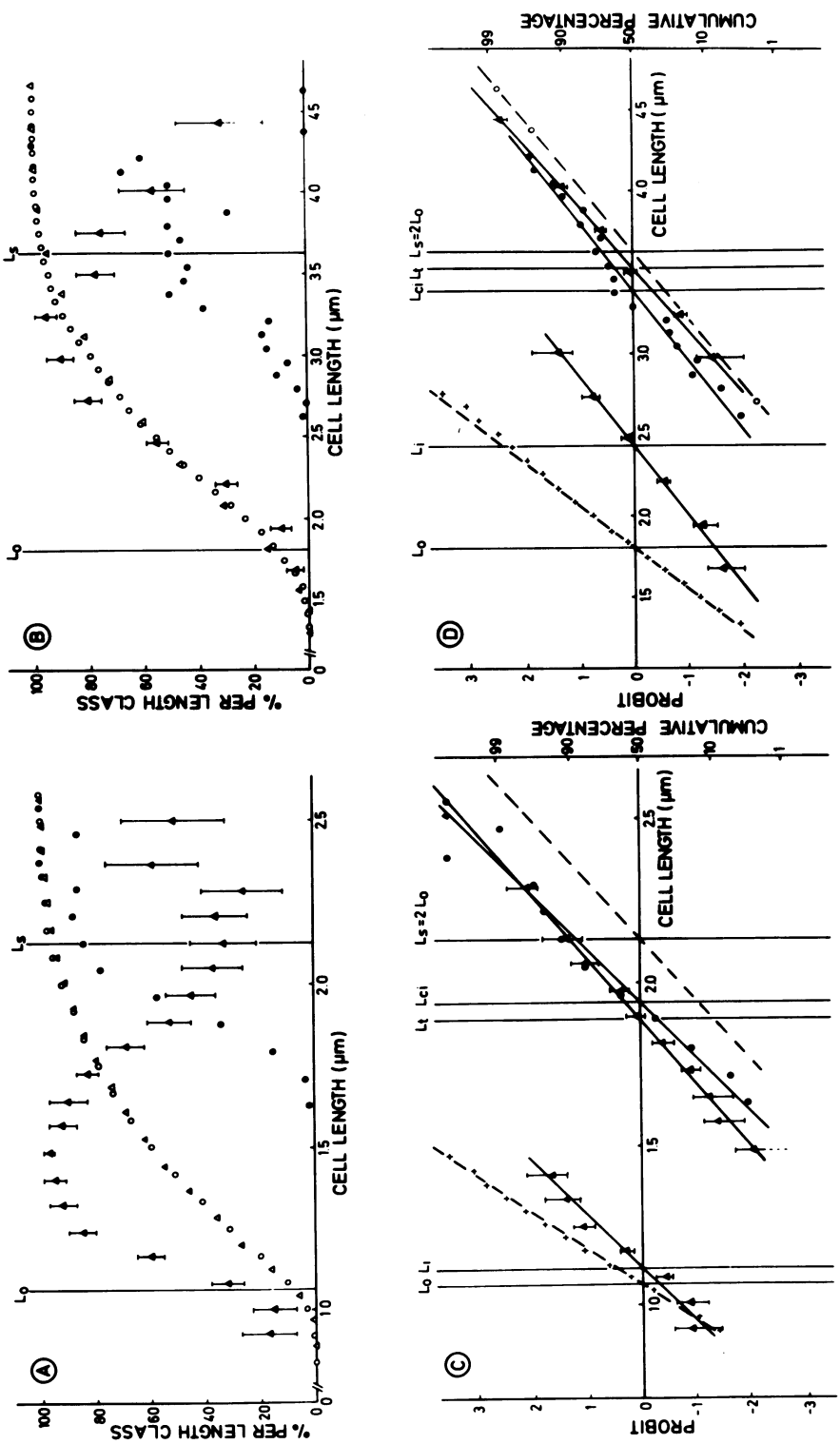

FIG. 2. *(A) and (B) Cumulative length distributions and percentages of radioactive and constricted cells in each length class. (A) E. coli B/r A; τ = 109 min. (B) E. coli B/r K; τ = 100 min. (△) Cumulative distribution of pulse-labeled and radioautographed cells after multiplication of cell length with the factor f (Table 2). (○) Cumulative distribution of control cells. (▲) Percentages of radioactive cells in each length class; SD is given by flags. (●) Percentages of constricted cells in each length class. The average lengths of newborn (L_o) and separating (L_s) cells are indicated by vertical lines. (C) and (D) Cumulative length distributions of cells at successive events in the cell cycle, plotted on probability paper. (C) E. coli B/r A. (D) E. coli B/r K. The percentages of radioactive and constricted cells observed in each length class (A and B) were corrected as explained in the Appendix, parts i and ii, and plotted on probability paper. The lines calculated by linear regression represent the cumulative length distributions of cells at initiation and termination of DNA replication (▲) and at initiation of cell constriction (●). Broken lines indicate the cumulative length distributions of newborn and separating cells. Crosses (+) represent the cumulative distribution of newborn cells calculated by making use of the distribution of the ratio between lengths of daughter and mother cells (see Fig. 3). Average lengths at which events occur are indicated by vertical lines (see Table 1 for symbols).*

for a number of experiments. It should be noted that the data on lengths at initiation and termination have now been corrected for the duration of the [^{3}H]thymidine pulse (see Appendix, part iii). In all experiments shown in Table 3, the SD of cell lengths increased most dramatically between cell birth (L_o) and initiation of chromosome replication (L_i) and remained relatively constant during the rest of the cycle. The same result is indicated by the slopes of the lines in Fig. 2C and D, the slopes being inversely proportional to the SD. One would expect the SD of newborn cells to be half that of dividing cells, if cells divide in equal halves. Because of the asymmetry in cell division (as shown in Fig. 3), the SD at L_o is higher than half the SD at L_s

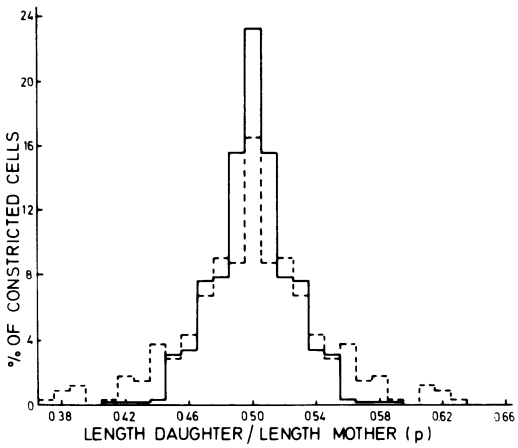

FIG. 3. *Frequency distributions of the ratio p = length of daughter cell/length of mother cell. p was calculated by dividing the distance between cell pole and site of constriction by the total length of the constricted cell. Because the sum of the lengths of the daughters must equal that of the mother, the average of the measured distribution and the distribution in reverse with respect to the vertical line p = 0.5 is represented. Continuous line: E. coli B/r A, τ = 109 min; coefficient of variation, 5%. Broken line: E. coli B/r K, τ = 100 min; coefficient of variation, 9%.*

(Table 3). It will further be observed that, in strain B/r A, termination of DNA replication precedes constriction, whereas in strains B/r K and F26 these processes more or less coincide (Fig. 2C and D and Table 3).

Relationship between length and age in the cell cycle. The measurements can give information on the kinetics of growth during the division cycle in two ways. First, the duration of periods devoid of DNA synthesis can be calculated from the percentage of unlabeled cells at the beginning (*B* period) and at the end (*D* period) of the distributions by making use of the formula for the ideal age distribution of an exponentially growing population (19). Likewise, the *T* period can be calculated from the percentage of constricted cells. The average cell lengths found for the different events (Table 3) and the calculated periods have been indicated in a length-time diagram (triangles in Fig. 4).

For the second approach, the average rate of elongation in each length class was calculated by means of the analysis of Collins and Richmond (2). For this purpose, use has been made of the cumulative distributions of extant (Fig. 2A and B), newborn, and separating cells (dashed lines in Fig. 2C and D). The average age of each length class was calculated by integrating the rates of elongation over the shorter lengths (10). The results have been plotted in the same length-time diagram (points in Fig. 4). It is evident from Fig. 4 that in both substrains most of the points as well as the triangles fall on the straight line (solid lines in Fig. 4) representing exponential increase of length with average age. Such a mode of elongation is in accordance with the finding by radioautography (7, 31) of an exponential increase in the macromolecular mass of individual cells during the cell cycle.

Assuming exponential length increase, the average durations of the *B*, *C*, and *D* periods have been calculated from the average cell lengths in Table 3, and they have been summarized in Table 4. In general, the results in Table 4 con-

TABLE 3. *Average lengths and SD at different events during the cell cycle*[a]

Strain	τ (min)	Event									
		Cell birth		Initiation of DNA replication		Termination of DNA replication		Initiation of cell constriction		Cell separation	
		L_o	SD	L_i[b]	SD	L_t[b]	SD	L_{ci}	SD	L_s	SD
B/r A	109	1.00	0.10	1.03	0.14	1.74	0.15	1.81	0.15	2.00	0.17
B/r A	135	1.00	0.10	1.02	0.16	1.56	0.17	1.88	0.15	2.00	0.17
B/r K	100	1.00	0.14	1.31	0.21	1.92	0.18	1.87	0.23	2.00	0.22
B/r K	210	1.00	0.14	1.33	0.22	1.89	0.19	1.90	0.20	2.00	0.20
B/r F26	240	1.00	0.12	1.27	0.21	1.86	0.22	1.83	0.21	2.00	0.21

[a] For comparison between different experiments, all values were divided by L_o. See Table 1 for symbols used.
[b] Cell lengths at the events of initiation and termination of DNA replication were corrected for the duration of the pulse (see Appendix, part iii).

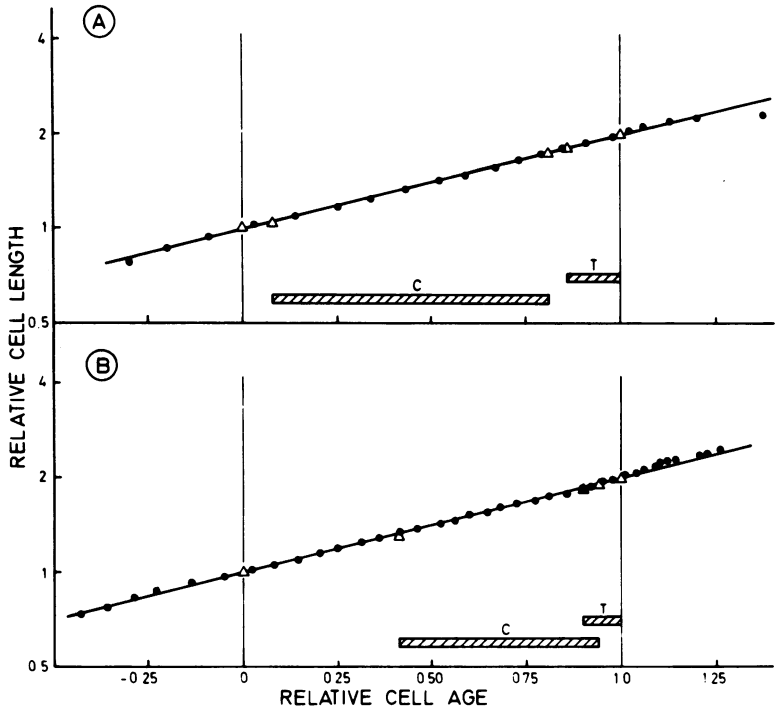

FIG. 4. *Plots of cell length versus average cell age. (A) E. coli B/r A; τ = 109 min; (B) E. coli B/r K; τ = 100 min. (△) Average cell lengths (Table 3) at the beginning and end of the average B, D, and T periods calculated from the percentages of unlabeled cells at the beginning and end of the length distribution (Fig. 1) and from the percentage of constricted cells. (●) Cell length as a function of average age calculated from the length distributions of extant, newborn, and separating cells by means of the Collins and Richmond principle (2). Average cell lengths have been divided by L_0; average age at length L_0 has been fixed at 0 and that at length L_n at 1. Beginning and end of the cell cycle are indicated by vertical lines. The hatched bars represent the durations of chromosome replication (C) and cell constriction (T).*

TABLE 4. *Average duration of different periods in the cell cycle*[a]

Strain	τ (min)	Period			
		$\bar{B}$[b] (min)	$\bar{C}$[b] (min)	$\bar{D}$[b] (min)	$\bar{T}$[c] (min)
B/r A	109	5	82 (75)[d]	22 (38)	16
B/r A	135	4	83 (88)	48 (47)	15
B/r K	100	39	55 (53)	6 (17)	10
B/r K	210	86	106 (110)	17 (27)	16
B/r F26	240	83	132 (126)	25 (23)	27

[a] See Table 1 for symbols used.

[b] $\bar{B}$, $\bar{C}$, and $\bar{D}$ periods calculated from L_i and L_t in Table 3, assuming exponential length increase (see Fig. 4).

[c] $\bar{T}$ period calculated from the percentage of constricted cells in Table 2.

[d] Values in parentheses are from Helmstetter and Pierucci (Fig. 3 in ref. 12).

firm the DNA replication pattern reported previously (12): a considerable gap in DNA synthesis occurs in the B/r K and F26 strains in constrast to B/r A. In addition, the *D* period in the former strains is about equal to or even smaller than the *T* period (see Discussion).

Rate of DNA replication. To see whether the rate of DNA replication changes with the size of the cell, the average number of grains per cell in each length class was estimated from the slopes of the grain distribution plots transformed according to Hanawalt et al. (9; cf. 13, 32). The results, represented in Fig. 5, show that the average number of grains per cell increases about 32% during the cell cycle in strain B/r A and about 23% in strain B/r K, suggesting that large cells have a higher incorporation rate than small cells. It should be noted that the variation is not gradual as suggested by the calculated regression lines in Fig. 5. A jump occurs about halfway along the cycle, the significance of which is not known. If no intermittent stops occur during chromosome replication (13), the observed variation in incorporation rate may suggest a variation in the duration of the *C* period for cells of different sizes (see Discussion).

Cell volume at initiation of DNA replication. The determination of average length at initiation of DNA replication allows calculation of volume ($\bar{V}_i$) at initiation. The results from four independent experiments with strains B/r

A and K, grown under steady-state conditions with roughly the same doubling time, are summarized in Table 5. The value of $\bar{V}_i$ obtained for B/r K cells (0.46 μm^3) is higher than that found for B/r A cells (0.32 μm^3). For *E. coli* B/r H266, a strain closely resembling B/r K with respect to cell shape and DNA replication pattern (results not shown), a $\bar{V}_i$ of 0.43 μm^3 was obtained. Since strains B/r A and K have a different shape and a different DNA replication pattern, the possibility exists that these differences are also reflected in the respective initiation volumes.

DISCUSSION

Pattern of DNA replication and cell elongation in B/r substrains. The duration of the respective periods calculated from the radioautographic data for the three B/r substrains (Table 4) are in good agreement with the values reported by Helmstetter and Pierucci (12). In some experiments, however, the *D* periods tended to be shorter than the values of these authors and, in two cases (Table 4), even appeared shorter than the corresponding *T* period. This is not in accordance with our previous observations that *D* always exceeded *T* in slowly growing B/r A and K cells (27). The present results could be explained if some residual division occurred during processing of the pulse-labeled population (see Table 2). This would lead to a decrease in the percentage of unlabeled cells at the end of the cycle and, therefore, to a shorter *D* period.

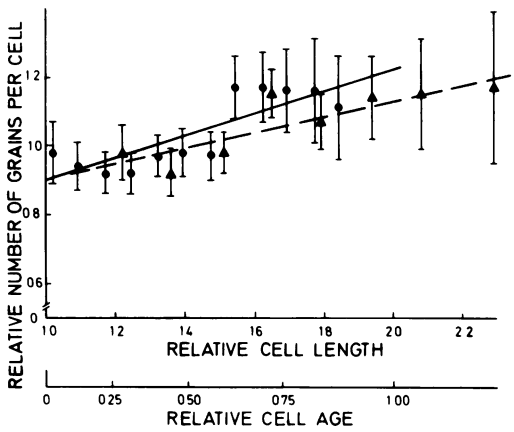

FIG. 5. *Rate of [^{3}H]thymidine incorporation as a function of cell length. The distribution, P(n), of the number of grains per cell (n) in each length class was plotted as the frequency function H(n) = ln[P(n)·n!] versus n. The average number of grains per cell was estimated from the slope of the regression line through H(n) with n ≥ 1 and is represented in arbitrary units (1 unit = average grain count of radioactive cells in the total population) as a function of relative length (1 unit = L_o). (●) E. coli B/r A (τ = 109 min; continuous line); (▲) E. coli B/r K (τ = 100 min; broken line). The lines were obtained by linear regression. Standard error is indicated by flags.*

Helmstetter and Pierucci (12) observed a decreasing quality of synchronous growth for the three substrains in the order of F26, A, and K. On the basis of the ratio of the SD of the lengths of newborn and separating cells (Table 3), in which the asymmetry of cell division is reflected, the substrains can be placed in the same order.

Unlike the observations of Helmstetter and Pierucci (12), our results (Table 5) suggest that the volume at initiation of chromosome replication is different in B/r substrains A and K. The value for $\bar{V}_i$ of about 0.45 μm^3 obtained for the comparable strains B/r K and H266 is higher than the 0.35 μm^3 estimated for H266 from the relationship between cell width and doubling time under the assumption of linear elongation (model 2 in ref. 8). The present values depend solely on the accuracy of the dimensional measurements. As compared to living cells observed by phase-contrast microscopy (magnification, ×4,000) the cell widths of slow-growing B/r A and K cells (τ = 160 min) prepared by agar filtration were found to be about 10% smaller in both strains.

The finding of an exponential mode of length increase for both B/r substrains A and K (Fig. 4) is in accordance with the previous observation (27) that their length distributions have the same shape and suggests that the mode of elongation in these particular cases is independent of the pattern of DNA replication (cf. 5). The results in Fig. 4 further imply that cells continue to elongate during the constriction process. The

TABLE 5. *Average volume of cells at initiation of DNA replication*

Strain	τ (min)	$\bar{L}$[a] (μm)	$2\bar{R}$[a] (μm)	$\bar{V}$[b] (μm^3)	$\bar{V}_i$[c] (μm^3)
B/r A	117[d] (8)	1.57 (0.15)	0.59 (0.04)	0.44 (0.08)	0.32 (0.06)
B/r K	107 (10)	2.57 (0.16)	0.49 (0.03)	0.48 (0.07)	0.46 (0.07)

[a] Average lengths ($\bar{L}$) and widths ($2\bar{R}$) were determined from cells prepared by agar filtration.

[b] Average volume ($\bar{V}$) was calculated from $\bar{L}$ and $2\bar{R}$, assuming the shape of cells to be that of right cylinders.

[c] Average volume ($\bar{V}_i$) at initiation of DNA replication was calculated from $\bar{V}$ by multiplication with the ratio $L_i/\bar{L}$. This ratio was fixed to 0.746 for the A strain and 0.954 for the K strain, as can be derived from Table 2 and 3.

[d] All data are averages of four independent experiments; numbers in parentheses are the corresponding SD.

exponential mode of elongation (or constant specific growth rate) is, however, at variance with the more complex growth kinetics derived previously by means of the Collins and Richmond principle (2) from size distributions measured with the light microscope (2, 31) and with the Coulter Counter (10). In both cases the specific growth rate was found to increase between divisions. This discrepancy may be ascribed to errors in the measurement of size distributions. In this respect it can be noted that, in contrast to the size distributions obtained by light microscopy (2, 31) or with the Coulter Counter (10), our length distributions show a shoulder on the right side of the distribution (see Fig. 1). The shoulder is also present in theoretical distributions calculated by assuming exponential growth and a coefficient of variation of size at division of 10% (see Fig. 1 in ref. 13). Because a similar shoulder is observed in volume distributions obtained from unfixed *E. coli* cells using a Coulter Counter with an improved detector (30), we believe that our length distributions determined from air-dried cells are fairly accurate.

Are initiation of DNA replication and cell division coordinated? In the three different B/r substrains that have been compared in the present study, the standard deviation of cell lengths has been shown to increase between birth and initiation of DNA replication and to remain relatively constant between initiation and cell separation (Fig. 2C and D; Table 3). The coefficient of variation at initiation of DNA replication was found to be about 16%, which is in accordance with the value derived by Koch (13) from the data of Chai and Lark (1) and of F. Forro (unpublished; quoted by Koch). Koch raised the question (13) of whether the variation in size at initiation of DNA replication is sufficiently precise to serve as a control for cell separation; in other words, whether or not there can be a direct correlation between these two events. We will discuss the two possibilities (see Fig. 6) with the assumption that cells elongate in an exponential way (Fig. 4). In addition, length at initiation of constriction (L_{ci}) is considered rather than length at cell separation (L_s), assuming both events to be tightly coupled. With respect to the time interval, we thus consider the $C + D - T$ period instead of the $C + D$ period.

If size at initiation of constriction is independent of size at initiation of DNA replication, both small and large cells at age a_i (open symbols, Fig. 6) will initiate cell constriction at an average length L_{ci}. The SD of L_{ci} will then be independent of that of the length at initiation of DNA replication (L_i). The finding of a similar SD for L_i and L_{ci} (Table 3) would thus be fortuitous. As

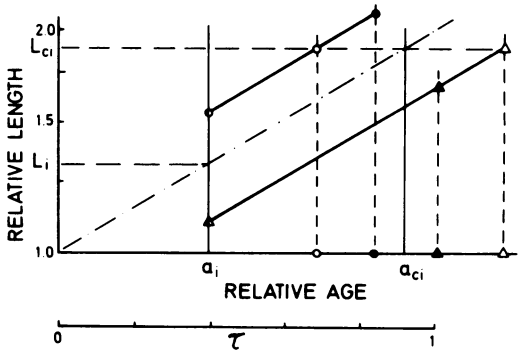

FIG. 6. *Length versus age. As an example, parameters applying to B/r K cells were taken. Individual cells have been assumed to elongate exponentially. Triangles and circles at age a_i indicate cells that initiate DNA replication at a small size (L_i − SD) and a large size (L_i + SD), respectively. Open symbols: size at constriction independent of size at initiation of DNA replication. Closed symbols: size at constriction dependent on size at initiation (constant size increment during $C + D - T$). The variation in a_{ci} and thus in the $C + D - T$ period is indicated by the symbols on the abscissa.*

can be seen from Fig. 6, individual cells which initiate chromosome replication at a small length (open triangles; L_i − SD) have to accrue more to reach L_{ci} than cells which initiate at a large length (open circles; L_i + SD). This leads to a pronounced variation in the $C + D - T$ period, as indicated by the open symbols on the abscissa in Fig. 6.

If size at initiation of constriction is dependent on size at initiation of DNA replication, the finding of a similar standard deviation for L_i and L_{ci} can be explained by an identical size increment during the $C + D - T$ period for both small and large cells at age a_i (closed symbols, Fig. 6). The variation in the $C + D - T$ period, as indicated by the closed symbols on the abscissa in Fig. 6, will be small as compared to the variation obtained in the case of independent events (open symbols).

To distinguish between the two possibilities mentioned above, the variation in the $C + D - T$ period has to be known. Our finding of a small variation (10 to 15%) in the rate of DNA synthesis during the cell cycle (Fig. 5) does not seem to be compatible with the rather large variation in $C + D - T$ expected for independently controlled sizes (Fig. 6, open symbols). We therefore interpret the observed constancy of the SD of cell lengths after initiation of DNA synthesis (Table 3) as indicative for a direct correlation between chromosome replication and cell division (Fig. 6, closed symbols).

Koch (13) has stated that if $C + D$ were

rigorously constant, then the size at initiation should be closely correlated with the size of the same cell at cell division; in addition, the two sizes should have identical coefficients of variation. On the basis of computer simulations made to fit the radioautographic data of Chai and Lark (1), Koch concluded that "initiation is much less well controlled than cell division, and therefore initiation cannot control or time cell division" (13). The best fit was obtained for a coefficient of variation of the size at initiation of DNA replication of 15%, which is similar to our observations. When defining his condition for correlated events (i.e., the coefficient of variation of cell size has to remain constant, or, in other words, the standard deviation has to increase during the cell cycle), Koch (13) assumed that the cell grows exponentially. However, when $C + D$ is not rigorously constant, but negatively correlated with size at initiation (Fig. 6, closed symbols), or alternatively, when cells grow linearly, cell size at initiation and at cell division can be closely correlated (same size increment) while the standard deviation between the two events remains the same (Table 3).

A constant C period is suggested by the observations of Zusman and Rosenberg (32). They found by means of radioautography with the light microscope that the rate of DNA synthesis was independent of the size of *Myxococcus xanthus* cells. Likewise, Koch (13) concluded from his analysis of the unpublished data of F. Forro that individual cells of *E. coli* replicate their DNA at very nearly the same rate independent of cell size. By contrast, our observations on the rate of thymidine incorporation (Fig. 5) show a variation of 10 to 15% in the rate of DNA synthesis during the cell cycle. Because knowledge of the variation of time intervals in the cell cycle is important to further establish the correlation between DNA synthesis and cell division, experiments are in progress to assess the variability of the $C + D - T$ period in synchronized cultures.

In conclusion, the present results indicate that the *E. coli* cell cycle may contain a dependent sequence of events in which DNA replication and cell division are coordinated. The existence of such a deterministic phase in the cell cycle has also been proposed by Smith and Martin (25) to occur in the cell cycle of eucaryotic cells as well as of bacteria (Martin and Smith, personal communication).

APPENDIX

(i) Calculation of the percentage of cells per length class which have terminated DNA replication. In Fig. 7A the observed percentage of radioactive cells per length class (r) is schematically represented as a function of cell length on probability paper (solid line). If $\Omega - \theta$ are, respectively, the percentages of cells per length class which have initiated and terminated DNA replication, and L_t^{min} is the minimum cell length at which termination of DNA replication occurs, then $r = \Omega$ applies to length classes with $L \leq L_t^{min}$, and a regression line through the data points yields the cumulative distribution of cells that initiate DNA replication (Ω; dashed line). $r = \Omega - \theta$, applies to length class $L > L_t^{min}$, and θ is calculated from r and the extrapolated Ω. After the correction discussed below (ii), θ is plotted on probability paper, and the regression line represents the cumulative length distribution of cells which terminate DNA replication.

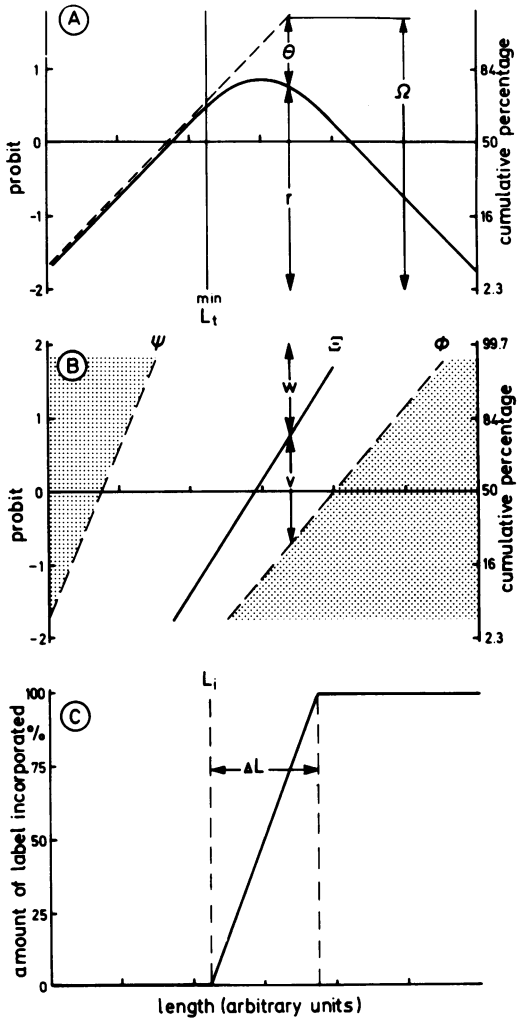

FIG. 7. *Schematic diagrams to illustrate the corrections explained in the Appendix and carried out to construct Fig. 2C and D and Table 3.*

(ii) Correction for depletion of length classes as a result of cell separation. In one particular length class, the number of cells that have proceeded through either DNA termination or constriction initiation will be equal to the observed number plus the number of cells which have disappeared from that

length class because they have already proceeded through cell separation. Figure 7B shows schematic representations of the cumulative length distributions of newborn (Ψ) and separating (Φ) cells (dashed lines) and of cells which are either terminating DNA replication or initiating cell constriction (Ξ; solid line) on probability paper. The observed percentage of cells per length class that have terminated DNA replication or initiated cell constriction (i.e., cells which have not yet proceeded through cell separation), will be equal to $100 \times v/(v + w)$ or $100 \times (\Xi - \Phi)/(1 - \Phi)$. From this formula the corrected percentage of cells per length class that have passed the event Ξ can be calculated. The determination of Φ has been described in the text.

(iii) Correction for the duration of the period of pulse-labeling. If L_i is the length at which cells will initiate DNA replication and ΔL is the average increase in length of cells during a pulse, then all cells with length between $L_i - \Delta L$ and L_i at the start of the pulse will initiate DNA replication. At the end of the pulse, these cells will have grown to lengths between L_i and $L_i + \Delta L$ and will have incorporated the amount of label indicated by the solid line in Fig. 2C. Therefore, after the Poisson analysis as carried out to obtain Fig. 2C and D, the average length found for initiation of DNA replication will be observed at $L_i + 1/2\ \Delta L$ and the standard deviation will have increased by about $1/3\ \Delta L$. Assuming exponential growth, ΔL can be calculated from $\Delta L = L_i \cdot (\ln 2 \times \Delta t/\tau)$, in which Δt is the duration of the pulse. The same reasoning applies for termination. In Table 2 the lengths (L_i, L_t) and their SD, as derived in the manner indicated in Fig. 2, have been diminished with, respectively, $1/2\ \Delta L$ and $1/3\ \Delta L$.

ACKNOWLEDGMENTS

This work has been greatly stimulated by discussions with A. L. Koch. We thank C. R. M. Koopmans and R. W. H. Verwer for useful suggestions in making the corrections given in the Appendix, G. J. Brakenhoff for his help with computer calculations, and N. B. Grover for his comments on the manuscript. The technical assistance of J. H. D. Leutscher, M. A. de Jong, and J. Joosten is gratefully acknowledged.

LITERATURE CITED

1. **Chai, N.-C., and K. G. Lark.** 1970. Cytological studies of deoxyribonucleic acid replication in *Escherichia coli* 15 T⁻: replication at slow growth rates and after a shift-up into rich medium. J. Bacteriol. **104**:401–409.
2. **Collins, J. F., and M. H. Richmond.** 1962. Rate of growth of *Bacillus cereus* between divisions. J. Gen. Microbiol. **28**:15–33.
3. **Cooper, S., and C. E. Helmstetter.** 1968. Chromosome replication and the division cycle of *Escherichia coli* B/r. J. Mol. Biol. **31**:519–540.
4. **Donachie, W. D., and K. J. Begg.** 1970. Growth of the bacterial cell. Nature (London) **227**:1220–1225.
5. **Donachie, W. D., K. J. Begg, and M. Vicente.** 1976. Cell length, cell growth and cell division. Nature (London) **264**:328–333.
6. **Donachie, W. D., N. C. Jones, and R. T. Teather.** 1973. The bacterial cell cycle. Symp. Soc. Gen. Microbiol. **23**:9–44.
7. **Ecker, R. E., and G. Kokaisl.** 1969. Synthesis of protein, ribonucleic acid, and ribosomes by individual bacterial cells in balanced growth. J. Bacteriol. **98**:1219–1226.
8. **Grover, N. B., C. L. Woldringh, A. Zaritsky, and R. F. Rosenberger.** 1977. Elongation of rod-shaped bacteria. J. Theor. Biol. **54**:243–248.
9. **Hanawalt, P. C., O. Maaløe, D. J. Cummings, and M. Schaechter.** 1961. The normal DNA replication cycle. II. J. Mol. Biol. **3**:156–165.
10. **Harvey, R. J., A. G. Marr, and P. R. Painter.** 1967. Kinetics of growth of individual cells of *Escherichia coli* and *Azotobacter agilis*. J. Bacteriol. **93**:605–617.
11. **Helmstetter, C. E., and S. Cooper.** 1968. DNA synthesis during the division cycle of rapidly growing *Escherichia coli* B/r. J. Mol. Biol. **31**:507–518.
12. **Helmstetter, C. E., and O. Pierucci.** 1976. DNA synthesis during the division cycle of three substrains of *Escherichia coli* B/r. J. Mol. Biol. **102**:477–486.
13. **Koch, A. L.** 1977. Does the initiation of chromosome replication regulate cell division? Adv. Microb. Physiol. **16**:49–98.
14. **Koch, A. L., and M. Schaechter.** 1962. A model for the statistics of the cell division process. J. Gen. Microbiol. **29**:435–454.
15. **Koppes, L. J. H., N. Overbeeke, and N. Nanninga.** 1978. DNA replication pattern and cell wall growth in *Escherichia coli* PAT 84. J. Bacteriol. **133**:1053–1061.
16. **Kopriwa, B. M.** 1973. A reliable, standardized technique for ultrastructural electron microscopic radioautography. Histochemie **37**:1–17.
17. **Kopriwa, B. M.** 1975. A comparison of various procedures for fine grain development in electron microscopic radioautography. Histochemistry **44**:201–224.
18. **Kubitschek, H. E., D. Valdez, and M. L. Freedman.** 1972. Efficiency of thymidine incorporation in *Escherichia coli* B/r as a function of growth rate. J. Bacteriol. **110**:1208–1210.
19. **Paulton, R. J. L.** 1970. Analysis of the multiseptate potential in *Bacillus subtilis*. J. Bacteriol. **104**:762–767.
20. **Powell, E. O.** 1964. A note on Koch and Schaechters's hypothesis about growth and fission of bacteria. J. Gen. Microbiol. **37**:231–249.
21. **Previc, E. P.** 1970. Biochemical determination of bacterial morphology and the geometry of cell division. J. Theor. Biol. **27**:471–497.
22. **Pritchard, R. H.** 1974. On the growth and form of a bacterial cell. Philos. Trans. R. Soc. London Ser. B **267**:303–336.
23. **Sargent, M. G.** 1975. Control of cell length in *Bacillus subtilis*. J. Bacteriol. **123**:7–19.
24. **Siegel, S.** 1956. Nonparametric statistics for the behavioral sciences, p. 47. McGraw-Hill Kogakusha, Ltd., Tokyo.
25. **Smith, J. A., and L. Martin.** 1973. Do cells cycle? Proc. Natl. Acad. Sci. U.S.A. **68**:2627–2630.
26. **Ward, C. B., and D. A. Glaser.** 1971. Correlation between rate of cell growth and rate of DNA synthesis in *Escherichia coli* B/r. Proc. Natl. Acad. Sci. U.S.A. **68**:1061–1064.
27. **Woldringh, C. L., M. A. de Jong, W. van den Berg, and L. Koppes.** 1977. Morphological analysis of the division cycle of two *Escherichia coli* substrains during slow growth. J. Bacteriol. **131**:270–279.
28. **Zaritsky, A.** 1975. On dimensional determination of rod-shaped bacteria. J. Theor. Biol. **54**:243–248.
29. **Zaritsky, A., and R. H. Pritchard.** 1973. Changes in cell size and shape associated with changes in the replication time of the chromosome of *Escherichia coli*. J. Bacteriol. **114**:824–837.
30. **Zimmerman, U., J. Schulz, and G. Pilwat.** 1973. Transcellular ion flow in *Escherichia coli* B and electrical sizing of bacterias. Biophys. J. **13**:1005–1013.
31. **Zusman, D., P. Gottlieb, and E. Rosenberg.** 1971. Division cycle of *Myxococcus xanthus*. III. Kinetics of cell growth and protein synthesis. J. Bacteriol. **105**:811–819.
32. **Zusman, D., and E. Rosenberg.** 1970. DNA cycle of *Myxococcus xanthus*. J. Mol. Biol. **49**:609–619.